Exciplex Photophysics. V. The Kinetics of Fluorescence Quenching of Anthracene by *N,N*-Dimethylaniline in Cyclohexane

Man-Him Hui and William R. Ware*

Contribution No. 145 from The Photochemistry Unit, Department of Chemistry, University of Western Ontario, London, Ontario N6A 5B7, Canada.
Received October 6, 1975

Abstract: The photokinetics of the fluorescence quenching of anthracene by *N,N*-dimethylaniline has been investigated by fluorescence decay and steady state techniques. It has been found that the transient effects associated with diffusion-controlled reactions must be taken into account. The forward reaction is diffusion controlled and the kinetic behavior of the system is dominated by exciplex dissociation to yield its precursors and by the exciplex radiative transition. $\Delta G°$, $\Delta H°$, and $\Delta S°$ for the excited state equilibrium at 25 °C are −4.6 and −12.1 kcal/mol and −25.2 eu, respectively. The kinetic model commonly used for excimers and exciplexes appears to be obeyed with the stipulation that the time dependence of the rate constant for exciplex formation must be taken into account. Correction methods for transient effects are discussed.

I. Introduction

In nonpolar solvents, there is reason to believe that the kinetics of exciplex formation and disappearance follow an "excimer type" mechanism.[1-5] That is

$$A + h\nu \xrightarrow{I_a(t)} A^*$$

$$A^* + Q \underset{k_4}{\overset{k_3}{\rightleftharpoons}} AQ^* \xrightarrow{k_6} \text{"products"}$$

$$A^* \xrightarrow{k_1} A + h\nu_M \qquad A^* \xrightarrow{k_2} A \qquad AQ^* \xrightarrow{k_5} A + Q + h\nu_E$$

This reaction scheme gives rise to the following coupled differential equations:

$$\frac{d[A^*]}{dt} = I_a(t) - (k_1 + k_2 + k_3[Q])[A^*] + k_4[AQ^*] \quad (1)$$

$$\frac{d[AQ^*]}{dt} = k_3[Q][A^*] - (k_4 + k_5 + k_6)[AQ^*] \quad (2)$$

The equations give, for δ-pulse excitation,

$$[A^*](t) = C_1 e^{-\lambda_1 t} + C_2 e^{-\lambda_2 t} \quad (3)$$

$$[AQ^*](t) = C_3(e^{-\lambda_1 t} - e^{-\lambda_2 t}) \quad (4)$$

where

$$C_1 = \frac{\lambda_1 - k_4 - k_p}{\lambda_1 - \lambda_2}[A^*]_0 \quad (5)$$

$$C_2 = \frac{k_4 + k_p - \lambda_2}{\lambda_1 - \lambda_2}[A^*]_0 \quad (6)$$

$$C_3 = -\frac{k_3[Q]}{\lambda_1 - \lambda_2}[A^*]_0 \quad (7)$$

$$k_p = k_5 + k_6 \quad (8)$$

$$\lambda_{1,2} = \tfrac{1}{2}\{k_1 + k_2 + k_3[Q] + k_4 + k_p \pm \sqrt{(k_1 + k_2 + k_3[Q] - k_4 - k_p)^2 + 4k_3k_4[Q]}\} \quad (9)$$

Equation 9 gives the following relationships[6] for the λ:

$$\lambda_1 + \lambda_2 = k_1 + k_2 + k_3[Q] + k_4 + k_p \quad (10)$$

When $k_1 + k_2 > k_4 + k_p$,

$$\lim_{[Q]\to 0} \lambda_1 = k_1 + k_2 \quad (11)$$

$$\lim_{[Q]\to 0} \lambda_2 = k_4 + k_p \quad (12)$$

When $k_1 + k_2 < k_4 + k_p$,

$$\lim_{[Q]\to 0} \lambda_1 = k_4 + k_p \quad (13)$$

$$\lim_{[Q]\to 0} \lambda_2 = k_1 + k_2 \quad (14)$$

The following steady state equations can also be derived:

$$\Phi_M^0/\Phi_M = 1 + \left(\frac{k_3}{k_1 + k_2}\right)\left(\frac{k_p}{k_4 + k_p}\right)[Q] \quad (15)$$

$$\Phi_E/\Phi_M = \left(\frac{k_5}{k_1}\right)\left(\frac{k_3[Q]}{k_4 + k_p}\right) \quad (16)$$

The subscripts M and E refer to monomer and exciplex, respectively, while the superscript 0 refers to the situation when [Q] = 0.

The so-called Stern-Volmer "constant" is therefore given by:

$$K_{SV} \equiv (\Phi_M^0/\Phi_M - 1)/[Q] = \left(\frac{k_3}{k_1 + k_2}\right)\left(\frac{k_p}{k_4 + k_p}\right) \quad (17)$$

In actual fact there have been relatively few studies[3,4,7,8] of systems specifically selected to examine critically the validity of this model for exciplexes (as distinguished from excimers) and to establish not only values for all the rate constants but also all the activation parameters. A substantial fraction of the information currently available regarding exciplexes in nonpolar solvents is derived from steady state fluorescence measurements coupled with unquenched lifetimes.[2,9,10] Only a very limited number of studies[3,4,7,8] have been reported where the time dependences of the concentrations [A*] and [AQ*] were examined with sufficient precision, accuracy, and freedom from interfering effects to permit one to comment critically on the validity of the above model and evaluate even some of the rate parameters with confidence.

In the model presented above, there are six rate constants and in fact two (k_2 and k_6) in general represent more than one nonradiative process. Thus a rather extensive set of measurements is required to meet the goals set forth above.

This paper reports a reasonably comprehensive study of the system anthracene-*N,N*-dimethylaniline (DMA) in cyclohexane. Both steady state and transient studies have been conducted as a function of concentration and temperature.

When this work was initiated, the following questions seemed of particular significance:

(a) Does the above model account quantitatively for the growth and decay of AQ* and the decay of A* subsequent to pulsed excitation of A?

(b) What is the enthalpy of the formation reaction of AQ* from A* and Q and how does the value obtained from d ln $(k_3/k_4)/dT^{-1}$ compare with that calculated from steady state data in the conventional manner with a so-called Stevens-Ban plot[4,11] [ln $(\Phi_E/\Phi_M[Q])$ vs. $1/T$]?

(c) Critically related to (b) is the question, does k_5 vary with temperature?

(d) Do the steady state and transient measurements give a self-consistent quantitative account of the photokinetic behavior of the system?

(e) If we write $k_4 = A_4 \exp\{-(\Delta E_4^{\ddagger}/RT)\}$, how do the parameters A_4 and $\Delta E_4^{\ddagger}$ compare with the other two systems reported in the literature[7,8] and is the correlation suggested by Figure 6, ref 12, borne out by more data?

(f) Is the enthalpy of the formation reaction of AQ* from A* and Q consistent with known oxidation and reduction potentials and optical transition energies?[1,2,3,10]

This system is also of interest in view of the recent work of Chuang and Eisenthal[12] using picosecond laser techniques to follow the growth of the anthracene-DMA exciplex. In order to explain their data they found it necessary to explore corrections for the effects of diffusion and in fact obtained good agreement with the standard continuum model. Thus in seeking answers to the questions posed above the possibility of diffusion effects entering into the formulation was regarded as a distinct possibility. Chuang and Eisenthal also obtained the interaction distance for the forward quenching step which is an important parameter for corrections to the kinetic equations needed to describe the exciplex and monomer time evolution as well as the steady state quenching.

It is not uncommon for the rates of various processes in an exciplex system to be such that one cannot answer all of the above questions; the reason being an inability to obtain individual rate constants.[13] A critical test of the kinetic model is frequently impossible. However, the aromatic hydrocarbon-amine exciplexes are more amenable to comprehensive kinetic studies because of the presence, generally, of both monomer and exciplex emission sufficiently separated in average energy to permit the independent study of the behavior of both species, and because the monomer and exciplex lifetimes are generally quite different. A typical set of spectra is shown in Figure 1. The anthracene-DMA system is one such combination of a donor and acceptor.

II. Experimental Section

a. Transient Measurement. Fluorescence decay measurements were made on a time-correlated single photon counting instrument, details of which have been described elsewhere.[14-16] The excitation source was a Photochemical Research Associate's Nanosecond Flashlamp System. An Oriel G-772-3900 sharp cut-off filter was used in the measurement of the unquenched anthracene decay and also in the cases where it was not necessary to separate the monomer and exciplex fluorescence. A Balzers K − 1 broadband interference filter was used to measure monomer decay in the presence of quencher. Although this filter transmits a small amount of exciplex emission, the characteristics of the photomultiplier photocathode (bialkali type DU) reduce detection of exciplex emission even further. Finally, the exciplex emission was isolated by using an Oriel G-772-3900 filter followed by a Kodak Wratten No. 12 filter. The function of the first filter is to cut down short-wavelength radiation which might induce unwanted fluorescence in the Kodak-Wratten filter. All samples were excited at 340 nm. Temperature was regulated to ±0.1 °C using a thermostated cell holder.

As mentioned earlier, the exciplex scheme predicts that the decay law for the monomer fluorescence intensity should be of the form

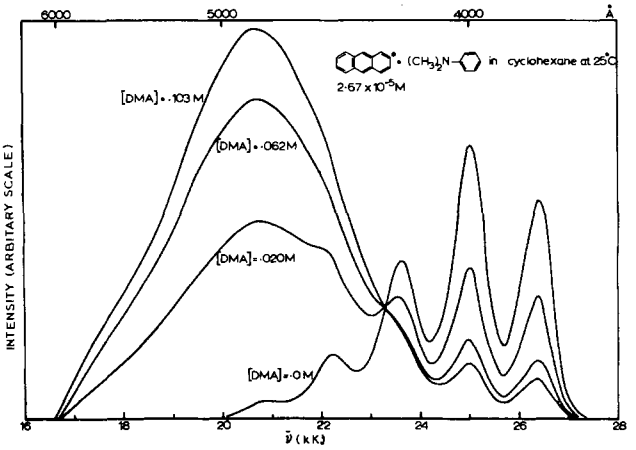

Figure 1. Corrected fluorescence spectra of anthracene + *N,N*-dimethylaniline in cyclohexane at 25 °C.

$$A_1 e^{-t/\tau_1} + A_2 e^{-t/\tau_2}$$

and that for the exciplex should be

$$A_3 (e^{-t/\tau_1} - e^{-t/\tau_2})$$

when k_3 is time independent. The constants A_i are related to the C_i through the appropriate radiative rate constants.

Therefore, even if the filtering system transmits some exciplex emission together with the monomer emission, the values obtained for τ_1 and τ_2 should not be affected; only the pre-exponential factor would change. However, in later sections it will be shown that k_3 is in fact time dependent.[17-20] As long as the initial portion of the decay curve was avoided in the analysis, the τ_1 value obtained (short-lived component) was independent of whether the Oriel G-772-3900 filter (monomer + some exciplex) or the Balzers K − 1 filter (mostly monomer) was used. Since the Oriel filter transmits much more light than the Balzers filter, it was used in many of the experiments.

Two time scales on the Time to Amplitude Converter (Ortec 437) were used. A short time scale was used when τ_1 was to be accurately measured. In this case, τ_2 could also be obtained, but only with a very large standard deviation. Therefore, a long time scale was used when τ_2 was to be accurately measured. Here, the decay law was assumed to be single exponential and only the later portion of the decay curve to which τ_1 does not contribute was analyzed. τ_2 was independent of which of the three filtering systems was used.

The decay curves were analyzed with the iterative convolution[14,15] method using the Marquardt algorithm[22] for least-squares estimation of nonlinear parameters consistent with the minimum on the χ^2 hypersurface. We believe that this is the best method presently available to analyze decay data from single photon counting instruments. (This will be discussed in detail in a later paper.[22]) To recover the shape of the response of the system to δ-pulse excitation from the observed fluorescence decay data and the observed lamp profile, the Exponential Series Method of Ware, Doemeny, and Nemzek was used.[16] The only modification was that the Marquardt method, rather than the usual analytical method, was used to search the parametric hypersurface. This appears to yield an improvement over the older method[16] as far as accuracy is concerned. To obtain actual rate parameters, a decay law of the form $A_1 e^{-t/\tau_1} + A_2 e^{-t/\tau_2}$ was assumed. The Marquardt algorithm was used again to find the best fitting values for A_1, τ_1, A_2, and τ_2, by iterative convolution with the lamp profile.

b. Steady State Measurement. Fluorescence spectra were measured on a conventional 90°, two-monochromator spectrofluorimeter equipped with a thermostated cell holder. Φ_M^0/Φ_M and Φ_E/Φ_M values were obtained with the same instrument. The intensities at 378 and 500 nm were taken as a measure of monomer and exciplex emission respectively to avoid interference from spectral overlap. Initially, the intensities were obtained from the spectra. Subsequently, the output from the micromicroammeter was fed directly to a digital voltmeter. With this modification, the measurements could be made within a relatively short time interval, thus avoiding the problem of lamp instability.

c. Chemicals. Zone-refined anthracene was used in all experiments. Additional purification by column chromatography produced no

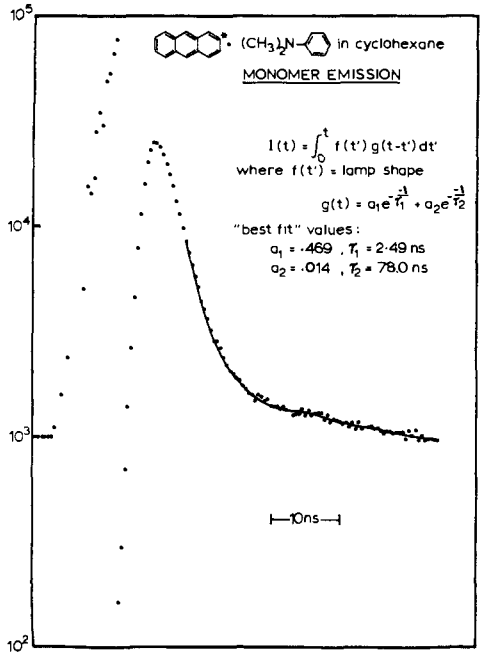

Figure 2. Typical monomer decay curve. [DMA] = 0.02 M, 34 °C.

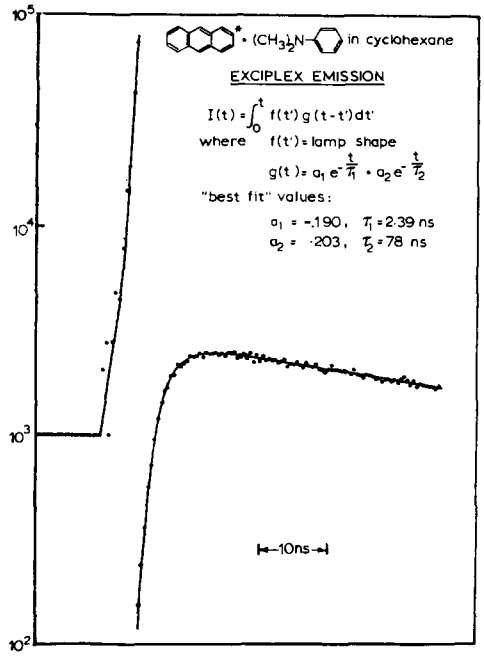

Figure 3. Typical exciplex decay curve. [DMA] = 0.02 M, 34 °C.

change in the measured lifetime. *N,N*-Dimethylaniline (Fisher) was purified by repeated trap to trap vacuum distillation in a grease-free, mercury-free vacuum line. Cyclohexane was purified by chromatography through a column of alumina. The concentration of anthracene in the samples was 2.7×10^{-5} M while that of *N,N*-dimethylaniline ranged from 0 to 0.1 M. All samples were degassed on a grease-free, mercury-free vacuum line.

III. Results and Discussion

a. Determination of Rate Constants. Experiments resulted in the following data: (a) the monomer and exciplex decay curves; (b) the Stern-Volmer constants for monomer fluorescence as a function of quencher concentration; and (c) the relative fluorescence quantum yields of monomer (Φ_M) and exciplex (Φ_E). These data were obtained in cyclohexane at five temperatures ranging from 14 to 42 °C.

The monomer decay law was strictly a single exponential in the absence of quencher, as indicated by the success of it-

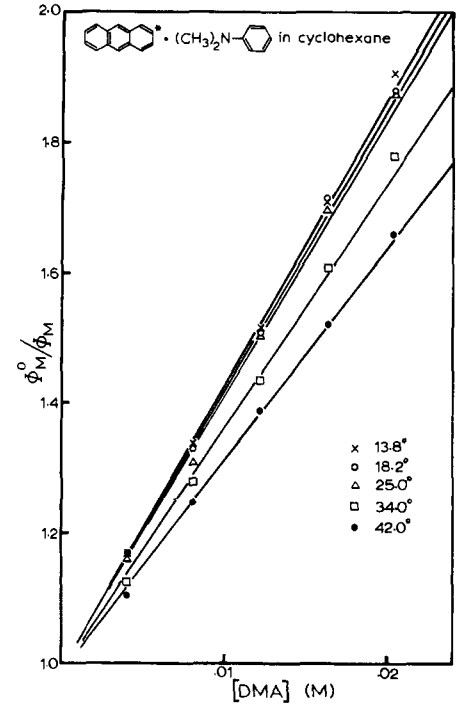

Figure 4. Stern-Volmer plots.

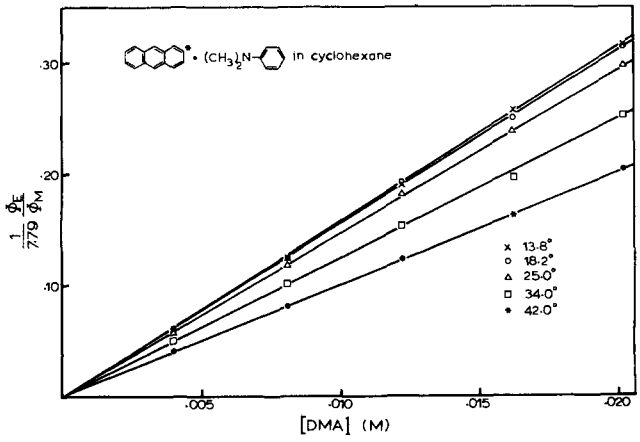

Figure 5. $(1/7.79)(\Phi_E/\Phi_M)$ vs. [DMA].

erative convolution over three decades. Upon the addition of dimethylaniline, pronounced curvature of log (I_M) vs. t was evident at all temperatures with a shape qualitatively corresponding to the sum of two exponential functions (see Figure 2).

The exciplex emission exhibited a growth followed by a decay which was qualitatively in accord with a decay law given by the difference of two exponentials. This is shown in Figure 3.

The Stern-Volmer plots were only very slightly curved upward. They exhibited a pronounced negative temperature coefficient, i.e., less quenching at higher temperatures, whereas the relative quantum yield plots Φ_E/Φ_M were linear, and also exhibited a negative temperature coefficient. The above behavior is qualitatively consistent with the conventional excimer or exciplex mechanism. Typical curves are shown in Figures 4 and 5.

The decay laws for the monomer and exciplex emission intensity should be proportional to [A*](t) and [AQ*](t) given by eq 3 and 4, respectively. That is

$$I_M(t) = A_1 e^{-\lambda_1 t} + A_2 e^{-\lambda_2 t} \quad (18)$$

$$I_E(t) = A_3(e^{-\lambda_1 t} - e^{-\lambda_2 t}) \quad (19)$$

The actual decay curve is distorted by the instrument response function and the lamp profile, i.e.,

$$I_M^{obsd}(t) = \int_0^t I_M(t-t')I_L(t')\,dt' \quad (20)$$

$$I_E^{obsd}(t) = \int_0^t I_E(t-t')I_L(t')\,dt' \quad (21)$$

where $I_L(t)$ is the lamp profile distorted by the detection system.[14-16]

Quantitative agreement between the above model and the decay data was poor, as illustrated by the following observations:

(a) The experimental data for the monomer decay did not fit well the decay law given by eq 18. Yet, if one analyzed the data choosing a starting point for deconvolution further and further away from the initial portion of the curve, the fit became better and better. At the same time, λ_1 and λ_2 changed in magnitude, but the change decreased gradually as the fit improved. As mentioned earlier in the experimental section, a separate determination of λ_2 was made in which a long time scale was employed. λ_2 determined in the above experiments fell within experimental error of the long time scale measurements if and only if the initial portion of the decay curve was avoided. $\lambda_1 + \lambda_2$ was, however, a linear function of [Q].

(b) The exciplex decay in fact fit reasonably well to a decay law of the form

$$I_E(t) = A_3e^{-\lambda_1 t} + A_3'e^{-\lambda_2 t} \quad (22)$$

but $A_3' \neq -A_3$. Furthermore, the short-lived lifetime, $\tau_1 = 1/\lambda_1$, was consistently smaller than that obtained from the monomer decay. The long-lived component was very close to that obtained from measurements on a long time scale. $\lambda_1 + \lambda_2$ from the exciplex decay was linear with [Q] but had a significantly larger slope and intercept than $\lambda_1 + \lambda_2$ from the monomer decay. We note in passing that λ_1 is strongly dependent on the position of the rising edge of the exciplex curve.

(c) Attempts to calculate k_p from the intercept of $\lambda_1 + \lambda_2$ (from the monomer decay) and eq 15 failed, giving in some cases negative rate constants.

The excimer–exciplex model given above ignores transient effects associated with diffusion-controlled reactions.[17-20] That this might not be justified is suggested by the fact that $\Delta(\lambda_1 + \lambda_2)/\Delta[Q]$ is of the order of 10^{10} M^{-1} s^{-1} and $1 + (R'/\sqrt{\tau_0 D}) \cong 1.25$ for $R' = 7$ Å, $D = 2 \times 10^{-5}$ cm^2 s^{-1}, and $\tau_0 = 5$ ns. Also, the slight upward curvature of the Stern–Volmer plot was suggestive of transient effects.[20,23,24]

In order to properly examine the role transient effects might play in the quenching mechanism, it was necessary to consider the following coupled differential equations:

$$d[A^*]/dt = -(k_1 + k_2 + k_3(t)[Q])[A^*] + k_4[AQ^*] \quad (23)$$

$$d[AQ^*]/dt = k_3(t)[Q][A^*] - (k_4 + k_p)[AQ^*] \quad (24)$$

These two equations are similar to eq 1 and 2 with the exception that the constant k_3 is replaced by the full diffusion-controlled rate with transient terms given by eq 26. These must be solved simultaneously to obtain the impulse response functions $[A^*](t)$ and $[AQ^*](t)$. This does not appear possible to accomplish in closed form because of the variable coefficient $k_3(t)$ but the solution can be obtained numerically.[25] Once the impulse response functions are obtained, they may be integrated to infinity to give the steady state behavior Φ_M^0/Φ_M and Φ_E/Φ_M as a function of [Q] or convoluted with $I_L(t)$ to predict decay curves. Such an analysis permits one to examine the effect of the time evolution of $k_3(t)$ on both the decay and steady state behavior of this type of system.

The following approach was taken in order to circumvent the fact that k_4 and k_p were unknown, as were the parameters in $k_3(t)$:

(a) The monomer decay was analyzed by iterative convolution for various [Q] using only that portion of the decay curve somewhat removed from the maximum (toward long time). This yielded λ_1 and λ_2.

(b) From $\lim(\lambda_2)$, as $[Q] \to 0$, $k_4 + k_p$ was obtained (this is the correct limit for the present case where $k_1 + k_2 > k_4 + k_p$, see eq 13.

(c) From the indicial equation derived from eq 1 and 2

$$\lambda^2 - (k_1 + k_2 + k_3[Q] + k_4 + k_p)\lambda + (k_1 + k_2)(k_4 + k_p) + k_3k_p[Q] = 0 \quad (25)$$

k_p was calculated assuming $k_3 = \Delta(\lambda_1 + \lambda_2)/\Delta[Q]$ (see eq 10). The set $\{\lambda_i, [Q]_i\}$ yielded a set of $\{k_{pi}\}$. A weighted average was used to obtain the best value for k_p.

(d) k_4 was then estimated from $(k_4 + k_p) - k_p$.

(e) The values of k_1, k_2, k_4, and k_p were then used in eq 23 and 24 along with[17-20]

$$k_3(t) = \frac{4\pi RD_{AQ}}{1 + (D_{AQ}/\kappa R)}\left[1 + \frac{\kappa R}{D_{AQ}}e^{x^2}\,\mathrm{erfc}(x)\right] \quad (26)$$

where

$$x = \sqrt{D_{AQ}t}/[RD_{AQ}/(D_{AQ} + \kappa R)] \quad (27)$$

and

$$\mathrm{erfc}(x) = \frac{2}{\sqrt{\pi}}\int_x^\infty e^{-z^2}\,dz \quad (28)$$

The standard truncation[17,20] of $\exp(x^2)\,\mathrm{erfc}(x)$ was avoided in order to include the effects of the transient diffusional gradients during the initial few hundred picoseconds when [AQ*] is starting to increase. κ was calculated[17] from gas kinetics using

$$\kappa = k_{gas}/4\pi R^2 \quad (29)$$

with[17,20,23,26]

$$k_{gas} = 10^{-10}\ cm^3\ molecule^{-1}\ s^{-1}$$

R was then determined using $D = 1.75 \times 10^{-5}$ cm^2 s^{-1} and requiring that $R' = 7$ Å,[12,20,23] where

$$R' = R/[1 + (D_{AQ}/\kappa R)] \quad (30)$$

These values of R' and D were consistent with the values of k_3 obtained from

$$\Delta(\lambda_1 + \lambda_2)/\Delta[Q] \cong 4\pi R'DN'$$

where N' is the number of molecules per millimole. Through the use of numerical techniques for solving coupled first-order differential equations with variable coefficients, $[A^*](t)$ and $[AQ^*](t)$ were computed for a number of [Q] at 25 °C.

The following observations were made.

(a) Initially, [A*] fell more rapidly than predicted by eq 3 (computed using the same k_1, k_2, k_4, and k_p and setting $k_3 = 4\pi R'DN'$). The two curves subsequently crossed and then decayed with the same long-time constant. If [A*] was convoluted with a typical lamp, Gaussian noise added, and then λ_1 and λ_2 obtained by iterative convolution (assuming a double exponential decay law), values of λ_1 were obtained that were on average only 3% above those predicted by eq 9, provided the convolution avoided the initial decay portion of the curve. The time dependence of $k_3(t)$ appears responsible for the variation of λ_1 with the starting point of iterative convolution. In fact negligible errors are introduced if one avoids the initial decay of A* where $k_3(t)$ is rapidly changing with time. The 3% increase in λ_1 has an insignificant effect on the subsequent cal-

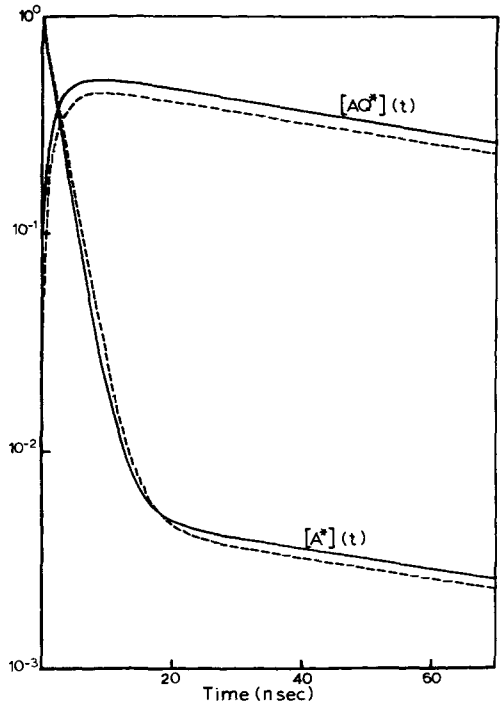

Figure 6. (—) Numerically generated [A*](t) and [AQ*](t) based on time-dependent $k_3(t)$ given by eq 26. (- - -) [A*](t) and [AQ*](t) based on constant k_3. $[A^*]_0$ assumed to be unit concentration.

culation of k_4 and k_p. A typical decay curve is shown in Figure 6.

(b) [AQ*](t) rises much more rapidly than predicted by eq 4 and remains above the predicted curve throughout the time range. Subsequently, both curves decay with the same long-time constant equal to that in (a). When [AQ*](t) was convoluted with a typical lamp curve, Gaussian noise added, and then the decay curve analyzed in the usual manner, the short-lived component obtained was indeed shorter than that obtained from the decay of [A*], an observation consistent with the experimental decay curves. These results justify ignoring the leading portion of the monomer decay in the analysis of the data as well as ignoring λ_1 obtained experimentally from the exciplex decay. It is important to note that one cannot avoid the leading portion of the exciplex decay in the analysis for both λ_1 and λ_2 because this is the only region where the short-lived component has an effect (see Figure 6).

(c) The numerically generated [A*](t) and [AQ*](t) obtained from solving eq 23 and 24 were integrated from zero to infinity using closed form equations to extrapolate the exponential tails. The results were most interesting. If one plots the calculated Φ_M^0/Φ_M vs. [Q], one obtains a very slightly curved plot with a slope that is within a few percent of the experimental value but 30% above that predicted by eq 15 (using values of k_1 through k_p determined as indicated above). Likewise, the Φ_E/Φ_M calculated from [A*](t) and [AQ*](t) by integration gave agreement to within a few percent of the experimental value but the slope was also 30% above that calculated from eq 16.

This might have been expected since the k_3[Q] term appears in the same form on the right-hand sides of both $\Phi_M^0/\Phi_M - 1$ and Φ_E/Φ_M.

Also, the use of the limiting equation[20,23]

$$\lim_{[Q]\to 0}(K_{SV}) = K_{SV}^0 = \frac{4\pi R' D N'}{k_1 + k_2}\left(1 + \frac{R'}{\sqrt{\tau_0 D}}\right)\left(\frac{k_p}{k_4 + k_p}\right) \tag{31}$$

was found to give a good estimate of the observed K_{SV}^0.

To sum up, the time dependence of k_3 affects both the transient and steady state measurements. If one uses a proper method to analyze the decay curves (avoiding the initial period in which transient effects are greatest), rate constants can be obtained with reasonable accuracy. However, the data from steady state measurements are profoundly affected, as indicated by the 30% discrepancy noted above. Nevertheless, the numerical calculation gave us an indication as to the proper corrections to make. Treating the Stern-Volmer data as a straight line (a good approximation) and writing

$$\Phi_M^0/\Phi_M = 1 + \left(\frac{k_3'}{k_1 + k_2}\right)\left(\frac{k_p}{k_4 + k_p}\right)[Q] \tag{32}$$

k_3' can be calculated from the experimental curve. Substituting into

$$\Phi_E/\Phi_M = \left(\frac{k_5}{k_1}\right)\left(\frac{k_3'}{k_4 + k_p}\right)[Q] \tag{33}$$

the value of k_5/k_1 is obtained to a reasonable approximation. The justification for this procedure is found in the numerical calculations described above. Failure to make the above described correction would lead to a large error in k_5 or k_5/k_1.

Thus, by the above somewhat circuitous route, k_1 through k_6 can be calculated (k_6 from $k_p - k_5$). The results at five temperatures are shown in Table I.

To examine how well these rate constants fit the experimental data, they were substituted back into eq 9 to obtain τ_1 and τ_2. The results are plotted in Figures 7 and 8. It can be seen that the agreement is quite satisfactory.

Let us examine briefly what has been described above. First, it was argued that k_3 was in fact time dependent and therefore eq 23 and 24 were used instead of eq 1 and 2 to describe the system. Then, after obtaining λ_1 and λ_2 from the experiments, relations derived from eq 1 and 2 were used to calculate k_3, k_4, and k_p. Is this procedure valid? If so, what is the meaning of the k_3 value obtained?

In order to answer these questions, we have to examine how $k_3(t)$ changes with time. In the first hundred picoseconds or so it falls rapidly, but the decrease gradually slows at later times. After a few nanoseconds, $k_3(t)$ is still decreasing but now the rate of change is extremely slow. This continues until the microsecond region when $k_3(t)$ has essentially reached its limiting value. As the decrease of $k_3(t)$ diminishes, eq 1 and 2 and hence other equations derived from them become more and more valid. This is seen in the fact that the monomer decay curve can be well described by a double exponential decay as long as the initial portion of the curve is ignored. This was precisely what was done when λ_1 and λ_2 were obtained. Thus the above procedure is a valid method for obtaining rate constants.

As to the meaning of the k_3 value obtained, it is an average of $k_3(t)$ over the experimental time range but biased to longer times. In fact, it is only a few percent higher than the limiting value. But as mentioned before, this small error does not affect subsequent calculation of k_4 and k_p in any significant way. As to the calculation of thermodynamic constants and activation parameters such as $\Delta E^{\ddagger}$, which involve logarithms of rate constants, the error introduced is minimal.

It is interesting to compare the above with the case of static quenching. In the latter, it is assumed that A and Q form a complex in the ground state also. Therefore, upon excitation, A* is rapidly quenched by the Q to which it is bound thus giving rise to phenomena such as anomalously high Stern-Volmer constants and curved Stern-Volmer plots.[20,23,24] In the present case, the Q molecules which happen to be around A* will quench it in a very short time. Quencher molecules far away have to diffuse through the solvent to quench A*. These two cases may be differentiated when finite ground state

Table I. Rate Constants for the Quenching of Anthracene Fluorescence by *N,N*-Dimethylaniline in Cyclohexane[a]

Rate constant	Units	Temp, °C 13.8	18.2	25.0	34.0	42.0
$\Phi_M^{0\,b}$				0.30		
τ_M^0	ns	5.32 ± 0.04	5.27 ± 0.04	5.22 ± 0.04	5.17 ± 0.04	5.14 ± 0.04
k_1^c	ns^{-1}	0.0575	0.0575	0.0575	0.0575	0.0575
k_3	$l.\ mol^{-1}\ ns^{-1}$	7.74 ± 0.24	7.84 ± 0.25	9.36 ± 0.28	9.50 ± 0.36	11.7 ± 0.5
$\lim_{[Q]\to 0} \tau_2$	ns	97.0 ± 0.6	90.0 ± 0.8	77.5 ± 1.0	59.5 ± 1.5	42.5 ± 2.5
$k_4 + k_5 + k_6$	μs^{-1}	10.31 ± 0.04	11.11 ± 0.10	12.90 ± 0.17	16.81 ± 0.42	23.5 ± 1.4
$k_5 + k_6$	μs^{-1}	9.01 ± 0.08	9.06 ± 0.06	9.23 ± 0.07	9.69 ± 0.32	10.08 ± 0.19
k_4^d	μs^{-1}	1.30 ± 0.09	2.05 ± 0.12	3.68 ± 0.18	7.12 ± 0.53	13.4 ± 1.4
k_5	μs^{-1}	7.7 ± 0.5	7.6 ± 0.5	7.5 ± 0.5	7.3 ± 0.6	7.1 ± 0.8
k_6	μs^{-1}	1.3 ± 0.5	1.4 ± 0.5	1.8 ± 0.5	2.4 ± 0.7	2.9 ± 0.8
$\frac{d}{d[Q]}\left(\frac{1}{7.79}\frac{\Phi_E}{\Phi_M}\right)$	M^{-1}	15.7 ± 0.1	15.4 ± 0.2	14.7 ± 0.1	12.3 ± 0.2	10.0 ± 0.04
K_{SV}	M^{-1}	43.8 ± 1.7	43.2 ± 1.7	42.6 ± 1.6	37.9 ± 1.6	32.7 ± 1.5
K_{SV}^0	M^{-1}	39.5 ± 3.9	39.3 ± 3.8	36.7 ± 3.8	30.7 ± 3.7	28.0 ± 3.6
k_5/k_1^d		0.134 ± 0.008	0.132 ± 0.008	0.130 ± 0.008	0.126 ± 0.011	0.124 ± 0.014

[a] All errors quoted are standard deviations computed in conventional manner. [b] Φ_M^0 as a function of temperature was not determined because of the problems discussed by Ware and Baldwin[43] and because it had already been shown that in hexane, $k_1 \neq f(T)$.[43] [c] Assumed constant.[43] [d] k_1 assumed to be error free.

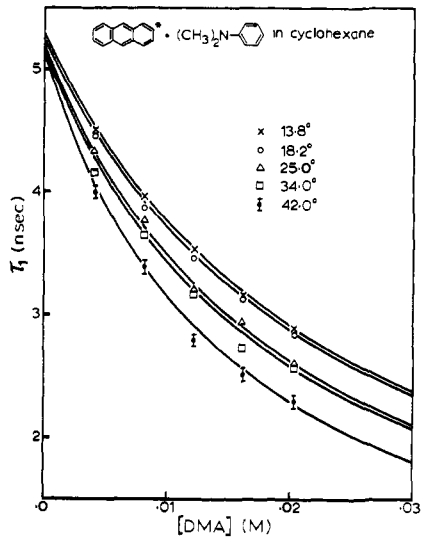

Figure 7. Comparison of experimental and calculated τ_1.

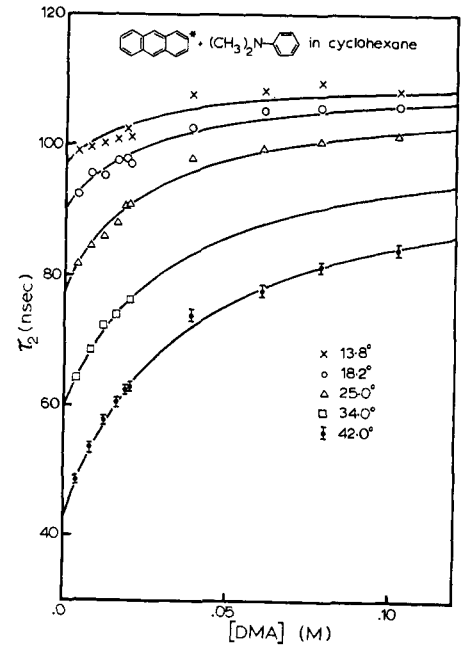

Figure 8. Comparison of experimental and calculated τ_2.

binding energy is present, as is discussed in detail in ref 20. There is no evidence for such complexes in the present system.

b. Discussion of Rate Constants. The radiative rate constant of A* was assumed to be constant and was calculated from the lifetime and the accepted quantum[1,27] yield at 25 °C. The values of k_3 tabulated in Table I are consistent with a diffusion-controlled forward reaction, although the actual probability may be slightly less than unity. From the data it is impossible to determine exactly the probability of exciplex formation during an encounter.

It is of interest to compare k_p and k_4. At 13.8 °C, k_p is only seven times k_4 and at 42 °C they are nearly equal with k_4, in fact, somewhat larger. Thus any attempt to ascertain the exciplex binding energy from a Stevens-Ban type plot [ln $(\Phi_E/\Phi_M[Q])$ vs. $1/T$] is doomed to failure because one cannot assume, even at 42 °C, that $k_4 \gg k_p$. Selinger and McDonald also have discussed the dangers associated with these plots.[28]

The quantum yield $k_5/(k_4 + k_5 + k_6)$ would be nearly unity if it were not for feedback, a situation which is understandable in nonpolar solvents but will surely change as one goes to polar media. From Table I it can be seen that at low temperatures $k_5 \gg k_6$ and in fact k_6 is too small to measure accurately. Only above 20 °C does k_6 become significant relative to k_5. This is consistent with the virtual absence of photochemical product formation in this system in nonpolar solvents as reported by Pac and Sakurai.[29] Also, it may well be that even at 42 °C, k_6 consists essentially of a nonradiative path or set of paths back to the ground state.

The radiative rate constant for the exciplex[8] is only about one-eighth that of the monomer. This is in sharp contrast to the pyrene-dimethylaniline exciplex[8] where k_5 is 2.5 times greater than k_1. This is probably related to the state mixings that occur as A* and Q come together which determine the

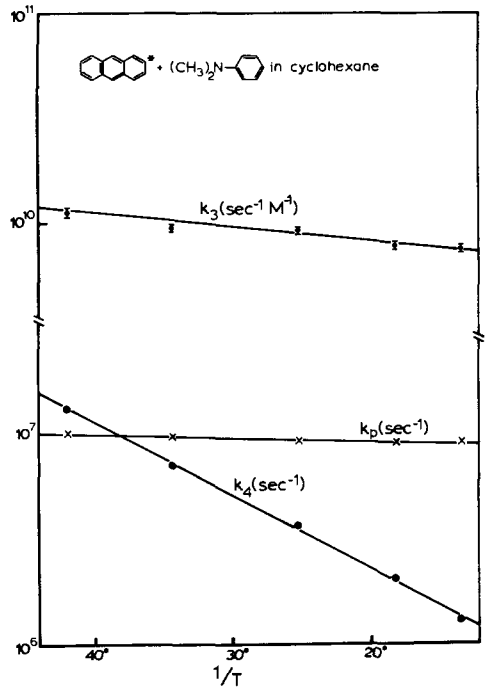

Figure 9. Arrhenius plots of k_3, k_4, and k_p.

ultimate magnitudes of various contributions to the total oscillator strength.

c. Activation Energies and Thermodynamic Properties. The activation energies associated with k_3, k_4, k_5, and k_6 are given in Table II. (See Figure 9.) The value obtained for k_3 is very close to what one would predict based on the known temperature coefficient of viscous flow in cyclohexane (2.5 ± 0.3 vs. 2.83 kcal for viscous flow).[30]

The feedback rate constant can be expressed as $k_4 = A_4 \exp\{-\Delta E_4^{\ddagger}/RT\}$, and from the data in Table I, one obtains log $A_4 = 17.3 \pm 0.5$ and $\Delta E_4^{\ddagger} = 14.6 \pm 0.7$ kcal. These values are in rough agreement with predictions based on Figure 6, ref 13. The $\Delta S^{\ddagger}$, $\Delta E^{\ddagger}$ correlation in exciplexes will be discussed below.

From the temperature coefficient of k_3/k_4 one obtains $\Delta H°$, the binding energy of the exciplex. The experimental value is −12.1 kcal and there is no evidence of a temperature dependence of $\Delta H°$. This absence of a temperature dependence would however be difficult to ascertain from log (k_3/k_4) vs. $1/T$, but one can argue on the basis of an assumed maximum ΔC_p for the exciplex equilibrium that over the temperature range in question an essentially constant $\Delta H°$ would be expected. Since $k_3/k_4 = \exp\{-\Delta G°/RT\}$ and $\Delta G° = \Delta H° - T\Delta S°$, one can calculate $\Delta G°$ and $\Delta S°$ for the exciplex excited state equilibrium from the data in Table I. The results are shown in Table III. The constancy of $\Delta S°$ over the temperature range is gratifying. Values of $\Delta S°$ of this magnitude have been observed[31] for strong CT ground state complexes such as I_2-$(CH_3)_3N$ and also for excimers.[1] Such large negative values for $\Delta S°$ suggest a quite rigid geometry in the exciplex state, but may also reflect solvent reorganization around the exciplex dipole.

The following empirical equation for $\Delta H°$ has been suggested by Weller[2]

$$\Delta H° = \Delta E_{0\text{-}0} - \Delta E_{1/2} - 0.15 \text{ eV} \qquad (34)$$

where $\Delta E_{0\text{-}0}$ is the energy of A → A* and $\Delta E_{1/2}$ is the difference in electrochemical oxidation potential of the donor and reduction potential of the acceptor in acetonitrile. From the absorption and emission spectra of anthracene in cyclohexane, one can estimate $\Delta E_{0\text{-}0} = 75.7$ kcal.[32] From the literature[33]

Table II. Activation Energies and Thermodynamic Properties (kcal/mol)

$\Delta E_3^{\ddagger}$	2.5 ± 0.3	$\Delta E_6^{\ddagger}$	5.4 ± 2.4
$\Delta E_4^{\ddagger}$	14.6 ± 0.7	$\Delta H°$	−12.1 ± 0.7
$\Delta E_5^{\ddagger}$	−0.5 ± 0.7	ΔH_R	4.4

Table III. Thermodynamic Quantities for the Excited State Equilibrium A* + Q ⇌ (AQ)*

	Temp, °C				
Quantity	13.8	18.2	25.0	34.0	42.0
$-\Delta G°$, kcal/mol	4.95	4.77	4.64	4.39	4.24
$-\Delta S°$, eu	25.1	25.3	25.2	25.2	25.1

one finds $\Delta E_{1/2} = 63.9$ kcal (anthracene −2.07 eV, DMA 0.70 eV vs. SCE). Thus $\Delta H° = 8.4$ kcal from these considerations. The $\Delta H°$ observed experimentally is 3.7 kcal higher than expected from the correlation. However, the data used by Weller to obtain the correlation represented by eq 34 have not been corrected for transient effects. They were obtained from the high-temperature slope of log $(I_E/I_M[Q])$ vs. $1/T$ plots. The transient effect (judging from $R'/\sqrt{\tau_0 D}$) is less serious at high temperatures because D increases with temperature.

Therefore, the $\Delta H°$ values used by Weller are expected to be somewhat low. Also, systematic errors associated with the assumptions involved in using Stevens-Ban[11] type plots must be considered. These may be the reasons for the small discrepancy between the $\Delta H°$ of this work and Weller's correlation. However, 3.7 kcal falls roughly within the standard deviation of ±0.1 eV associated with the correlation.[2]

From the conservation of energy, we have

$$E_{0\text{-}0} = \Delta H° + h\nu_{ct} + H_R \qquad (35)$$

where $h\nu_{ct}$ is the energy of the exciplex emission and ΔH_R is the ground state destabilization or repulsive energy between A and Q in the excited state geometrical configuration. From the experimental data $\Delta H_R = 4.4$ kcal. This value is similar to that obtained for other exciplexes.[8,10] For example, a value of 4.4 kcal is reported for the pyrene-DMA exciplex.[8]

It must be emphasized that the rate constants (k_3, k_4, and k_p) and their temperature coefficients discussed above were obtained without recourse to the data available from steady state quenching studies. Furthermore, the results of numerical integration of the coupled differential equations indicate that provided care is taken in selecting the appropriate portion of the monomer two-component decay curve for analysis, these rate constants are reasonably free from the effects of the transient terms of diffusion-controlled reaction-rate theory.

If the system in question were pulsed with a δ pulse of light to prepare A* and if k_1, k_2, and k_p were all zero, then the [A*] and [AQ*] would change with time as diffusion gradients were established and the random initial distribution of A and Q destroyed as the reaction proceeded. In a short period (~10^{-6} s) the system would reach a state where A* + Q ⇌ AQ* was established as a true equilibrium. The forward and backward rates would then closely correspond to k_3[A*][Q] and k_4[AQ*] respectively where k_3 and k_4 are, within experimental error, the values one obtains from lifetime measurements with due regard for corrections for transient effects in diffusion controlled reactions. Thus the $\Delta G°$ and $\Delta S°$ obtained are good approximations to the true properties of the excited state equilibrium.

Table I gives K_{SV}^0 as well as K_{SV}. The latter quantity represents the best straight lines drawn through slightly curved plots (see Figure 4). If instead one plots K_{SV} vs. [Q] in order

to account for this curvature, one obtains as intercepts the K_{SV}^0 value shown in Table I. These should, to a good approximation, exceed $4\pi R'DN'$ by the correction factor $(1 + R'/\sqrt{\tau_0 D})(k_p/[k_4 + k_p])$ where $\tau_0 = 1/(k_1 + k_2)$. While K_{SV}^0 is indeed smaller than the predicted corrected value (using $R' = 7$ Å and $D = 1.75 \times 10^{-5}$ s^{-1} cm^2), the correction appears to be slightly large. However, the curvature in the Φ_M^0/Φ_M vs. [Q] plot is so slight that K_{SV} as a function of [Q] shows considerable scatter. This gives rise to the large errors shown for K_{SV}^0 in Table I.

d. Quenching of Exciplex. A possible additional step in the photokinetic scheme must be considered, i.e., the quenching of AQ* by Q:

$$AQ^* + Q \xrightarrow{k_7} \text{product}$$

The principal question is, can this step explain the discrepancy between the steady state and lifetime measurements attributed above to the effects of diffusion control? The possibility that this step is significant has been investigated by calculating the effect of the added term $k_7[Q]$ to the steady state kinetics using the experimental data at 25 °C. It was found that if one let $k_7 = \alpha k_3$, an upper limit on α could be set at $\alpha < 0.005$ merely from the absence of curvature in the Φ_E/Φ_M plot vs. [Q]. That is, we now have

$$\Phi_E/\Phi_M = \left(\frac{k_5}{k_1}\right)\left(\frac{k_3[Q]}{k_4 + k_p + k_7[Q]}\right) \qquad (36)$$

which is quite sensitive to k_7 for rate constants in the range pertinent to this work. Only a small fraction of the discrepancy between the slope of Φ_M^0/Φ_M predicted by the lifetime measurements and that observed could be accounted for with $\alpha = 0.005$. Thus Φ_E/Φ_M is a much more sensitive parameter to test for exciplex quenching than Φ_M^0/Φ_M because the transient effects do not introduce significant curvature (vide supra).

Unfortunately, this test for the magnitude of k_7 is not sufficiently sensitive to rule out exciplex quenching by Q as an important step in the process involving AQ*. This can be seen by considering that if $\alpha = 0.005$ $k_7 \cong 5 \times 10^7$ m^{-1} s^{-1} and $k_7[Q]$ for [Q] = 0.1 M is 5×10^6 s^{-1}. This is of the same magnitude as k_4, k_5, and k_6. Further analysis is thus required.

Quenching of AQ* by Q does not influence the limit

$$\lim_{[Q]\to 0} (\lambda_2) = k_4 + k_p \qquad (37)$$

Thus a finite k_7 can change the relative magnitude of k_4 and k_p but not the sum as determined from eq 37. On the other hand, one has the limit

$$\lim_{[Q]\to \infty} \frac{\partial}{\partial[Q]} (\lambda_2) = k_7 \qquad (38)$$

Halpern[34] has used eq 38 to measure k_7, in a system where this type of quenching is important. Then, if $k_7 = 0$,

$$\lim_{[Q]\to \infty} \lambda_2 = k_p$$

and eq 38 gives a zero limit. Thus if k_7 is important, a plot of λ_2 vs. [Q] should curve upward at high [Q] and give a limiting slope equal to k_7. Also, τ_2 vs. [Q] should show a maximum, and λ_2 vs. [Q] a minimum. These predictions are not in accord with our observations, as can be seen in Figure 8. This last argument can be made more quantitative by introducing $k_7[Q]$ into eq 9 and calculating λ_2 for various k_4, α, and [Q]. This was done by setting $k_7 = \alpha k_3$. Then $\lambda_{1,2} = \frac{1}{2}[k_1 + k_2 + (1 + \alpha)k_3[Q] + k_4 + k_p] \pm [(k_1 + k_2 + (1 - \alpha)k_3[Q] - k_4 - k_p)^2 + 4k_3k_4[Q]]^{1/2}$. Since $(k_1 + k_2)$ and $(k_4 + k_p)$ were known, one could fix α and vary k_4 until the best fit to λ_2 vs. [Q] was obtained, as measured by a minimum in χ^2 for λ_2 vs. [Q]. α is now varied to produce a set of curves such as one shows in Figure 10. The best fit is for $\alpha \leq 10^{-5}$. For α between 10^{-4} and 10^{-5} there is also almost no effect on k_4 (or on k_p). Thus the quenching of AQ* by Q can be ignored, since $k_7[Q]$ appears to be much less than k_4, k_5, or k_6 for all [Q] used in these experiments.

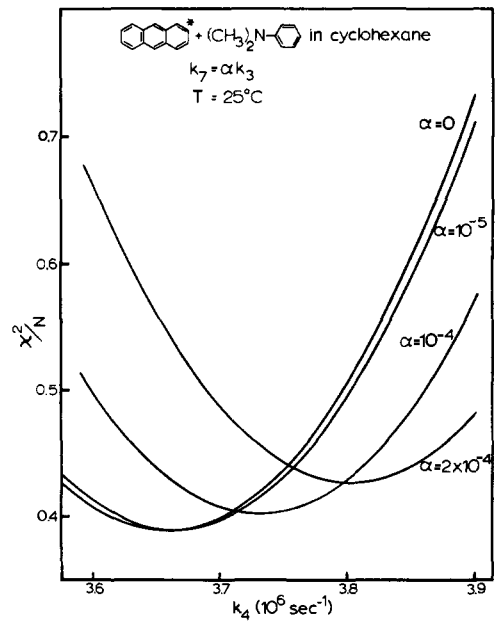

Figure 10. χ^2 vs. k_4 for a mechanism where the exciplex is quenched by Q.

e. The $\Delta S_4^{\ddagger} - \Delta E_4^{\ddagger}$ Correlation. There appears to be only five[7,8,35-37] exciplex systems in nonpolar solvents where both k_3 and k_4 have been measured by the analysis of fluorescence decay curves. These are perylene[7] and anthracene quenched by DMA (this work), pyrene quenched by DMA[35,36] and *N,N*-diethylamine (DEA),[8] and pyrene quenched by tributylamine[8,3] (TBA). However, only in two of these systems has the temperature coefficient of k_3/k_4 been directly measured by fluorescence decay measurements. In addition, there are a number of indirect measurements of k_3, k_3/k_4,[38] and its temperature coefficient using steady state measurements combined with unquenched or limiting lifetimes. These latter measurements are uncertain to an unknown extent due to (in some cases) transient effects of diffusion control and due to the possibility that the plot of $\ln(I_E/I_M[Q])$ vs. $1/T$ does not give a good approximation to ΔH° because $k_4 \approx k_p$. Nevertheless it is of interest to see if the correlation between $\Delta S^{\ddagger}$ and $\Delta E^{\ddagger}$ observed for excimers[13] holds for these exciplex systems.

For the systems where k_4 and $\Delta E_4^{\ddagger}$ were measured independently the required rates are directly available. The other systems to be considered fall into two classes: (a) k_3 and k_4 measured plus ΔH° (not necessarily by the same laboratory!); (b) k_3/k_4 and k_3 measured plus ΔH° (again not necessarily by the same lab). In all but one case $k_3 \cong k_{diff}$ and $\Delta E^{\ddagger}$ could be taken as the activation energy for diffusion. This gave $\Delta E_4^{\ddagger}$ from $\Delta H^\circ = \Delta E_3^{\ddagger} - \Delta E_4^{\ddagger}$ and then with k_4 one obtains A_4 in $k_4 = A_4 \exp\{-\Delta E_4^{\ddagger}/RT\}$. In one case $k_3 < k_{diff}$ but $\Delta E_3^{\ddagger}$ was measured along with ΔH°. Thus in this case also sufficient data were present for a comparison of $\Delta S_4^{\ddagger}$ and $\Delta E_4^{\ddagger}$. The numbers are presented in Table IV and in log A vs. $\Delta E_4^{\ddagger}$ plotted in Figure 11. The dispersion is normal for this type of correlation. The following points are of interest. (a) The line in Figure 11 lies slightly above that in Figure 6 of ref 13 and has a somewhat steeper slope. (b) From the slope, one can calculate an isokinetic temperature. From Figure 11 $T_{ISK} = 475$ K (from Figure 6, ref 13, $T_{ISK} = 582$ K). (c) The correlation of ΔH° and ΔS° for $A^* + Q \rightleftharpoons (AQ)^*$ is not as

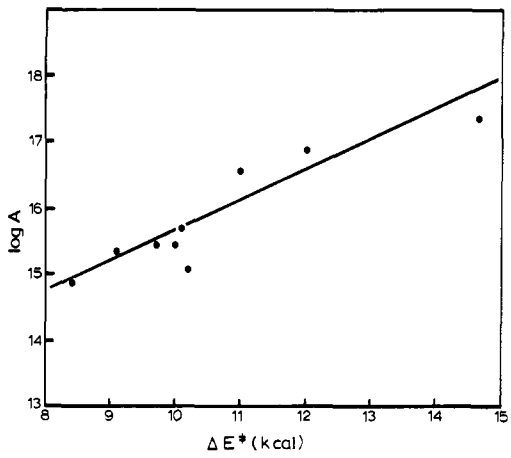

Figure 11. Correlation of log A_4 and $\Delta E_4^{\ddagger}$.

good. This is in contrast to the good correlation obtained for ground state CT[39] complexes (T_{ISK} = 427 K for amines with I_2). (d) TBA does not appear to fit the plot as well as the aromatic amines.

Person[40] has examined the question of the origin of the $\Delta S°$, $\Delta H°$ correlation for CT complexes. After examining the components of $\Delta H°$ and $\Delta S°$ from standard statistical mechanical equations, he concludes that the variation from compound to compound in $\Delta S°$ is mainly in ΔS_{vib}, the vibrational factor, and for $\Delta H°$, the variation is in $\Delta E_0{}^0$, the potential well depth. He then argues[41] that $\Delta S_{vib} \propto \Sigma \ln f_i$, where the f_i are force constants. An examination of the literature reveals that $\Delta E_0{}^0 \propto \ln f$ for diatomics in series such as HI, HBr, HCl, and HF. Thus Person concludes that the $\Delta H°$, $\Delta S°$ correlation has its origin in $\Delta E° \propto \ln f$. This same argument should be valid for the exciplex.

Since both the donor and acceptor vary in Figure 10, a high degree of correlation is not expected. The postulate $\Delta E_0{}^0 \propto \ln f$ may be better for the change to give the transition state than for the overall exciplex formation because the distance of separation is probably greater and a diatomic model might be expected to work better.

f. Conclusions. It is concluded that the experimentally observed kinetic behavior can be understood in terms of the conventional exciplex-excimer type photokinetic scheme provided one takes into account transient effects derived from the time evolution of concentration gradients. These latter effects manifest themselves on the leading edge of the monomer decay and for a short period after the decay curve has passed its maximum. The same effects are much more pronounced in the steady state measurements, in fact so significant that any attempt to calculate rate constants by combining steady state and decay time measurements without appropriate corrections may be doomed to failure (negative rate constants in some cases).

In this system the assumption that $k_4 \gg (k_5 + k_6)$ clearly fails and then one cannot obtain $\Delta H°$ from $I_E/I_M[Q]$. This may well be the case in a number of excimer and exciplex systems reported in the literature.[28] In many cases insufficient data were collected to establish whether or not this limit was indeed valid for the temperature range over which $\Delta H°$ was estimated. These difficulties may be avoided, along with most of the problems associated with diffusion control, if one obtains k_3 and k_4 from decay measurements alone.

The results in this publication provide us with essential background for further studies on the effects on mechanism and on individual rate constants of solvent polarity, steric hindrance, and electronic effects in A and Q. These areas are now under intensive investigation and the results will be submitted for publication in the near future. In addition, the effects of transient terms are being investigated for a variety of τ_0 and D for exciplex or excimer type photokinetics, as well as for diffusion-controlled quenching of A* and AQ* by an added quencher, such as O_2. The results will be submitted for publication in the near future.[42]

Table IV. $\Delta E_4^{\ddagger}$ and A_4, for Various D-A Pairs in Nonpolar Solvents, Calculated from Data Available in the Literature

	$\Delta E_4^{\ddagger}$, kcal	log A_4	Ref
Perylene-DMA	10.2	15.1	7
Anthracene-DMA	14.6	17.3	This work
Pyrene-DEA	10.8	16.6	8, 37
Pyrene-TBA	10.3	16.9	8, 36
Pyrene-DMA	9.7	15.5	34, 35
Anthracene-DEA	12.0	16.9	37
Pyrene-DEA	10.2	15.5	37
Dibenzanthracene-DEA	10.1	15.7	37
Perylene-DEA	8.4	14.8	37
Biphenyl-DEA	9.1	15.3	37

Acknowledgments. The authors wish to acknowledge the financial assistance of the National Research Council of Canada and the Army Research Office—Durham.

References and Notes

(1) J. B. Birks, "Photophysics of Aromatic Molecules", Wiley-Interscience, New York, N.Y., 1970. See also J. B. Birks, "Organic Molecular Photophysics", Vol. II, J. B. Birks, Ed., Wiley-Interscience, New York, N.Y., 1973, Chapter 9.
(2) A. Weller, "The Exciplex", M. Gordon and W. R. Ware, Ed., Academic Press, New York, N.Y., 1975.
(3) H. Beens and A. Weller, "Organic Molecular Photophysics", Vol. II, J. B. Birks, Ed., Wiley-Interscience, New York, N.Y., 1973, Chapter 4.
(4) B. Stevens, "Advances in Photochemistry", G. Hammond, J. Pitts, and W. Noyes, Jr., Ed., Wiley-Interscience, New York, N.Y., 1971.
(5) W. R. Ware, D. Watt, and J. D. Holmes, *J. Am. Chem. Soc.*, **96**, 7853 (1974). Paper I of this series.
(6) Equation 9 differs from eq 12 of paper I (ref 5) in the sign of the squared quantity under the square root. Normally this sign is of no consequence. However, it influences the way in which the limiting cases are stated. Equations 21 and 22 of ref 5 should be replaced with the more detailed limits given in eq 11-14 of this paper.
(7) W. R. Ware and H. P. Richter, *J. Chem. Phys.*, **48**, 1595 (1968).
(8) H. Nakashima, N. Mataga, and C. Yamanaka, *Int. J. Chem. Kinet.* **5**, 833 (1973), and references contained therein to earlier work.
(9) H. Beens and A. Weller, *Acta Physiol. Pol.*, **34**, 85 (1968); D. Rehm and A. Weller, *Isr. J. Chem.*, 8, 259 (1970); H. Knibbe, Thesis, University of Amsterdam, 1969.
(10) H. Beens, Thesis, University of Amsterdam, 1969.
(11) B. Stevens and M. I. Ban, *Trans. Faraday Soc.*, **60**, 1515 (1964). See also T. Forster and H. P. Spidel, *Z. Phys. Chem. (Frankfurt am Main)*, **45**, 58 (1965).
(12) T. J. Chuang and K. B. Eisenthal, *J. Chem. Phys.*, **62**, 2213 (1975); **59**, 2140 (1973).
(13) C. Lewis and W. R. Ware, *Mol. Photochem.*, **5**, 261 (1973).
(14) W. R. Ware, "Creation and Detection of the Excited State", Vol. IA, A. Lamola, Ed., Marcel Dekker, New York, N.Y., 1971, pp 213-302.
(15) C. Lewis, W. R. Ware, L. J. Doemeny, and T. L. Nemzek, *Rev. Sci. Instrum.*, **44**, 107 (1973).
(16) W. R. Ware, L. J. Doemeny, and T. L. Nemzek, *J. Phys. Chem.*, **77**, 2038 (1973).
(17) R. M. Noyes, *Prog. React. Kinet.*, **1**, 129 (1961).
(18) A. Weller, *Z. Physhem. (Frankfurt am Main)*, **13**, 335 (1957).
(19) A. H. Alwattar, M. D. Lumb, and J. B. Birks, "Organic Molecular Photophysics", Vol. I, J. B. Birks, Ed., Wiley-Interscience, New York, N.Y., 1973, pp 403-454.
(20) W. R. Ware and T. L. Nemzek, *J. Chem. Phys.*, **62**, 477 (1975).
(21) D. W. Marquardt, *J. Soc. Ind. Appl. Maths.*, **11**, 431 (1963); P. R. Bevington, "Data Reduction and Error Analysis for The Physical Sciences", McGraw-Hill, New York, N.Y., 1969.
(22) M. H. Hui, D. O'Connor, and W. R. Ware, paper in preparation.
(23) W. R. Ware and J. Novros, *J. Phys. Chem.*, **70**, 3246 (1966).
(24) W. R. Ware, P. R. Shukla, P. J. Sullivan, and R. V. Bremplis, *J. Chem. Phys.*, **55**, 4048 (1971).
(25) See, e.g., A. Ralston, "Numerical Methods for Digital Computers", A. Ralston and H. Wilf, Ed., Wiley, New York, N.Y., 1960, Chapter 8. The Subroutine HPCG from IBM System/360 Scientific Subroutine Package was used in the calculation.
(26) H. Knibbe, Thesis, University of Amsterdam, 1969.
(27) W. H. Melhuish, *J. Chem. Phys.*, **65**, 229 (1961); G. Weber and F. Teal, *Trans. Faraday Soc.*, **53**, 646 (1957). (See also ref 31.)
(28) R. J. McDonald and B. K. Selinger, *Mol. Photochem.*, **3**, 99 (1974); B. K. Selinger, *ibid.*, **1**, 371 (1969).

(29) B. K. Selinger, *Mol. Photochem.*, **1**, 371 (1969); C. Pac and H. Sakurai, *Tetrahedron Lett.*, **43**, 3829 (1969).
(30) J. Janz and R. P. T. Tomkins, "Non-Aqueous Electrolytes", Handbook, Vol. I, Academis Press, New York, N.Y., 1972, p 22.
(31) M. Tamres and J. Yarwood, "Spectroscopy and Structure of Molecular Complexes", J. Yarwood, Ed., Plenum Press, London, 1973, Chapter 3.
(32) I. B. Berlman, "Handbook of Fluorescence Spectra of Aromatic Molecules", Academic Press, New York, N.Y., 1971.
(33) Reference 29, Vol. II, 1973, pp 525–539.
(34) A. Halpern, *J. Am. Chem. Soc.*, **96**, 4382 (1974).
(35) K. Yoshihara, T. Kasuya, A. Inoue, and S. Nagakura, *Chem. Phys. Lett.*, **9**, 469 (1971).
(36) T. Okada, H. Matsui, H. Oohari, H. Matsumota, and N. Mataga, *J. Chem. Phys.*, **49**, 4717 (1968).
(37) N. Nakashima, N. Mataga, F. Ushio, and C. Yamanaka, *Z. Phys. Chem. (Frankfurt am Main)*, **79**, 150 (1972).
(38) H. Knibbe, D. Rehm, and A. Weller, *Ber. Bunsenges. Phys. Chem.*, **73**, 839 (1969).
(39) R. S. Mulliken and W. B. Person, "Molecular Complexes", Wiley-Interscience, New York, N.Y., 1969.
(40) W. B. Person, *J. Am. Chem. Soc.*, **84**, 536 (1962).
(41) A. Shepp and S. H. Bauer, *J.Am. Chem. Soc.*, **76**, 265 (1954).
(42) M. H. Hui and W. R. Ware, to be published.
(43) W. R. Ware and B. A. Baldwin, *J. Chem. Phys.*, **43**, 1194 (1965).

Kinetic Applications of Electron Paramagnetic Resonance Spectroscopy. 25. Radicals Formed by Spin Trapping with Di-*tert*-butyl Thioketone[1]

J. C. Scaiano[2] and K. U. Ingold*

Contribution from the Division of Chemistry, National Research Council of Canada, Ottawa, Ontario, Canada. *Received September 26, 1975*

Abstract: A variety of transient $R_nM\cdot$ radicals (M = C, Si, Sn, and P, but not O) have been trapped with di-*tert*-butyl thioketone and the persistent adduct radicals, $R_nMS\dot{C}(CMe_3)_2$ (**1**), have been examined by EPR spectroscopy. From a comparison of the hyperfine splittings by M in **1** and in $R_nMCH_2\dot{C}(CMe_3)_2$ and analogous radicals, and from a consideration of the *g* values for **1** (2.0024–2.0033), it is concluded that the R_nM group eclipses the C_α $2p_z$ orbital. Competitive experiments involving the reaction of *tert*-butyl with thione or oxygen at −80 °C and the reaction of methyl with thione or Me_3CNO at −40 °C indicate that alkyl addition to the thione has a rate constant of ca. 10^6 M^{-1} s^{-1} at these temperatures. The $CH_3S\dot{C}(CMe_3)_2$ radial exists in equilibrium with a dimer at temperatures in the range −70 to −110 °C: ΔH = 9.6 ± 1.5 kcal/mol; ΔS = 32 ± 3 gibbs/mol. Above −50 °C the $CH_3S\dot{C}(CMe_3)_2$ radical decays with the first-order kinetics. It is concluded that $CH_3S\dot{C}(CMe_3)_2$ and $SiH_3S\dot{C}(CMe_3)_2$ decay by an intramolecular transfer of H from M to C_α. The $CF_3S\dot{C}(CMe_3)_2$ radical is extremely persistent. The $(n\text{-}Bu)_3SnS\dot{C}(CMe_3)_2$ radical decays with second-order kinetics. Arrhenius parameters for some of the decay reactions are reported.

The carbon–sulfur double bond in thioketones is known to be a fairly good trap for carbon-centered[3-7] and sulfur-centered[6] free radicals.

$$R_nM\cdot + S{=}C< \rightarrow R_nMS\dot{C}<$$

This reaction appears to be important during the photolysis of thioketones in solutions containing good hydrogen donors, R_nMH.[5,6] The EPR spectra of a few $R_nMS\dot{C}Ar_2$ radicals obtained by the addition of carbon-centered radicals to thiobenzophenones have been reported.[5,6] Similar radicals have been produced by the reaction of simple alkyl Grignards (e.g., MeMgBr) with thiobenzophenone,[8] thiopivalophenone,[9a] 2,2,5,5-tetramethylcyclopentanethione,[9b] and thiofenchone.[9b] However, no detailed EPR spectroscopic study of carbon-centered or heteroatom-centered radical additions to dialkyl thioketones has yet been undertaken. For this reason, we have examined the reactions of a variety of transient radicals with di-*tert*-butyl thioketone. The adduct radicals produced, $R_nMS\dot{C}(CMe_3)_2$ (**1**), were generally quite persistent and gave excellent EPR spectra as we would expect from our earlier work on spin trapping with 1,1-di-*tert*-butylethylene[10-12] and di-*tert*-butylketimine.[13] We conclude from the EPR parameters of a variety of the adduct radicals that the R_nM group is in the eclipsed position with respect to the C_α $2p_z$ orbital. We have also measured the rate of trapping of transient carbon-centered radicals by this thione using competitive techniques and have studied the kinetics of decay of several **1**. A few experiments were also carried out with thiobenzophenone and adamantanethione.

Experimental Section

Di-*tert*-butyl thioketone was prepared from di-*tert*-butylketimine by reaction first with methyllithium and then with carbon disulfide according to the method of Barton et al.[14] It was purified by vacuum distillation and was stored under argon at −20 °C. Fortunately, the extinction coefficients of this thione (viz., λ_{max} 531 nm, ϵ 6.45 cm^{-1} M^{-1}; no other maxima until λ <275 nm; at 313 nm, ϵ 13.46) are low enough to allow the transient $R_nM\cdot$ radicals to be generated photochemically in its presence. The radicals were generated directly in the cavity of a Varian E-4 EPR spectrometer by previously described procedures.[11-13]

Thiobenzophenone[15] was prepared by reaction of benzophenone with gaseous H_2S and HCl. Adamantanethione was prepared by the method of Greidanus[16] from adamantanone and P_2S_5.

Results and Discussion

1. EPR Spectra. The EPR spectral parameters for the di-*tert*-butyl thioketone spin adducts are listed in Table I. Most of these radicals were quite persistent (see below) and their spectra were therefore sufficiently intense (see e.g., Figures 1, 2, 3, and 4) to observe splitting by magnetic nuclei in low natural abundance, e.g., ^{13}C, ^{29}Si, ^{119}Sn, ^{117}Sn, and even ^{33}S.

For any particular R_nM group, the hyperfine splittings by H_γ, $^{13}C_\alpha$, $^{13}C_\gamma$, and particularly M (see Table II) in the $R_nMS\dot{C}(CMe_3)_2$ radicals are very similar to the splittings found for the additions of the same $R_nM\cdot$ to di-*tert*-butylethylene,[12] i.e., **2**, and to di-*tert*-butylvinylidenetetramethylcyclopropane,[17] i.e., **3**. Since all **2** and **3** have the R_nM group in the eclipsed position with respect to the C_α $2p_z$ orbital we conclude that all **1** adopt the same eclipsed conformation.